

Supplement of Atmos. Chem. Phys., 18, 16139–16154, 2018
<https://doi.org/10.5194/acp-18-16139-2018-supplement>
© Author(s) 2018. This work is distributed under
the Creative Commons Attribution 4.0 License.



Atmospheric
Chemistry
and Physics
Open Access


Supplement of

Non-methane hydrocarbon variability in Athens during wintertime: the role of traffic and heating

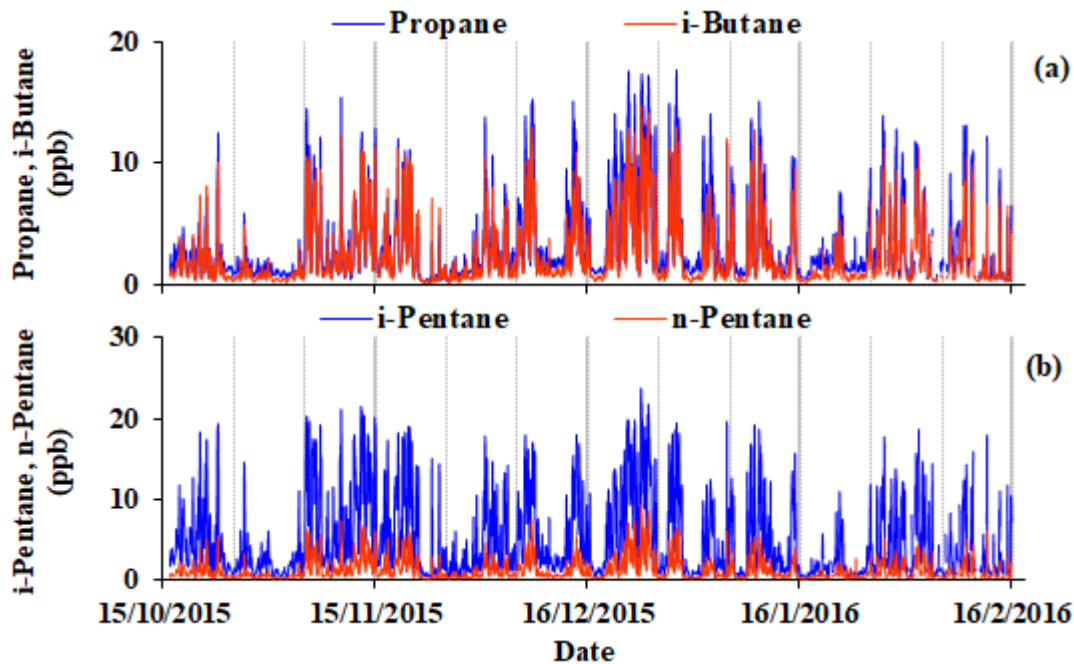
Anastasia Panopoulou et al.

Correspondence to: Eleni Liakakou (liakakou@noa.gr)

The copyright of individual parts of the supplement might differ from the CC BY 4.0 License.

Section S.1. Complementary figures.

Figure S1. Temporal variability of (a) propane and i-butane; and (b) i- and n - pentane based on hourly averaged levels for the period 16 October 2015 - 15 February 2016, at NOA's urban background site in Thissio, downtown Athens.

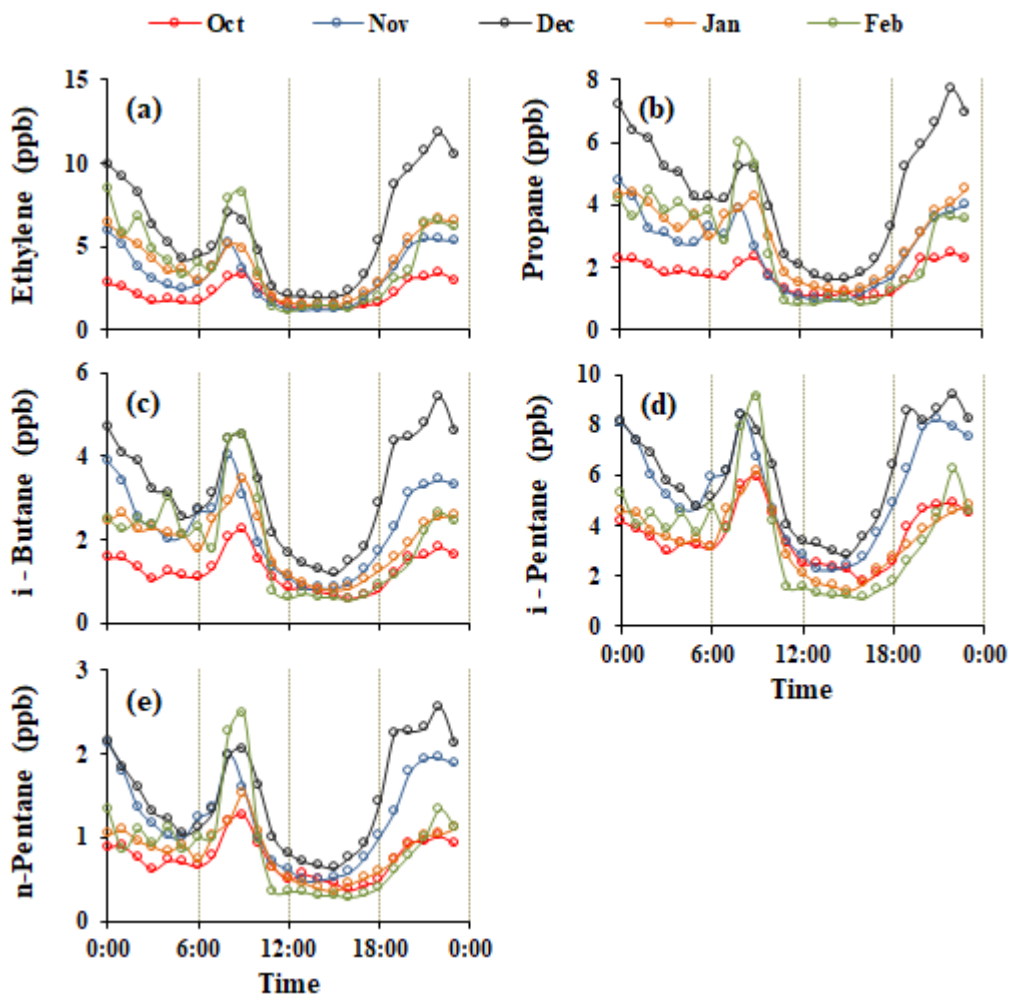


10

15

20

Figure S2. Monthly diurnal variability of (a) ethylene, (b) propane, (c) i-butane, (d) i-pentane and (e) n-pentane based on hourly averaged levels.



5

10

Figure S3. Correlation of (a) ethane, (b) ethylene, (c) propane, (d) propene, (e) i-butane, (f) i-pentane, (g) n-pentane, (h) isoprene, (i) CO, (j) BC, (k) BC_{wb} and (l) BC_{ff} relatively to wind speed for the period 16 October 2015 - 15 February 2016 at the Thissio urban background site.

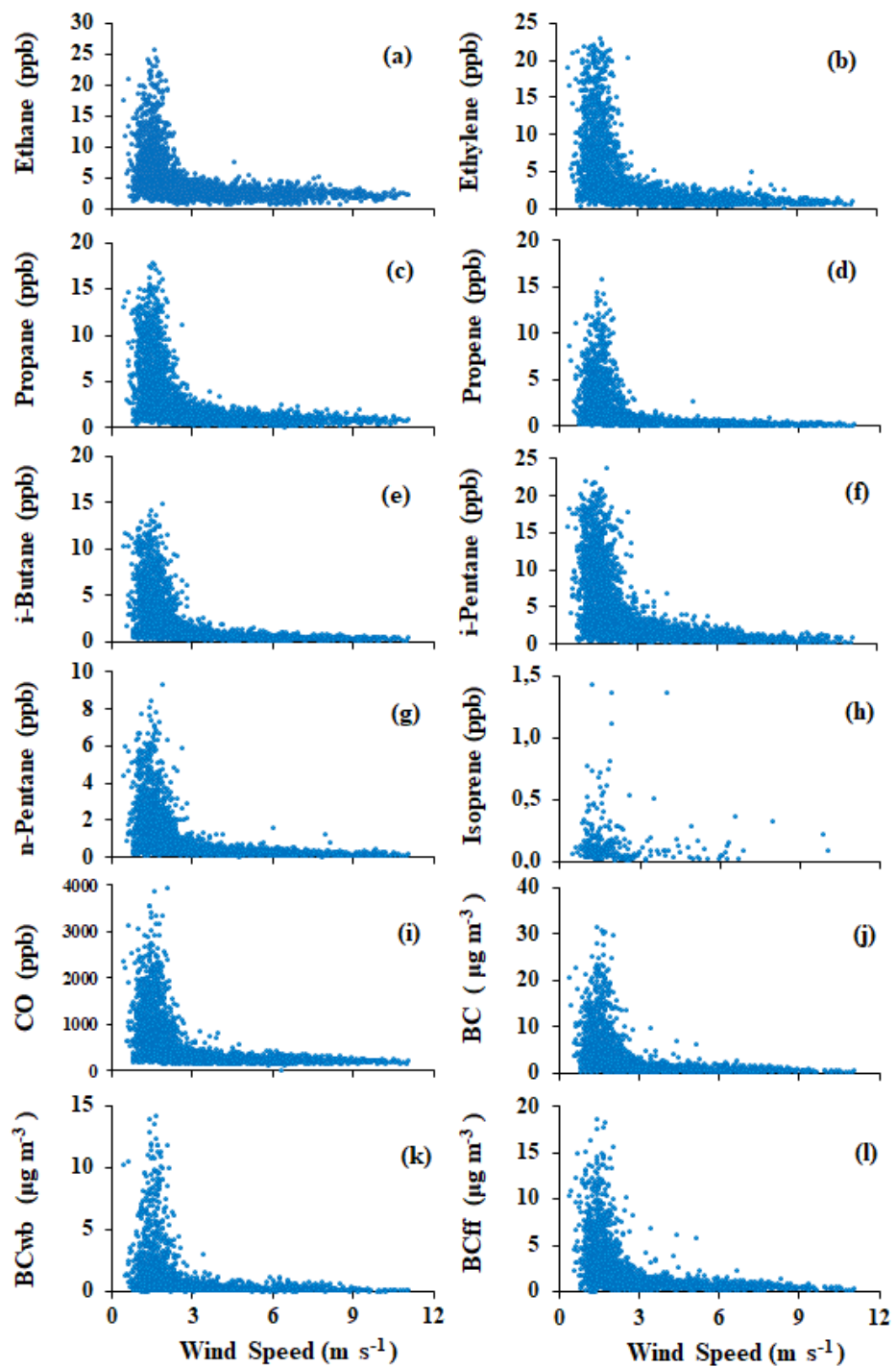


Figure S4. Wind rose (a) and concentration roses of (b) ethane, (c) ethylene, (d) propane, (e) propene, (f) i-butane, (g) i-pentane, (h) n-pentane, (i) isoprene, (j) toluene, (k) BC, (l) BC_{ff}, (m) BC_{wb}, (n) CO for the period 16 October 2015 - 15 February 2016 at the Thissio urban background site.

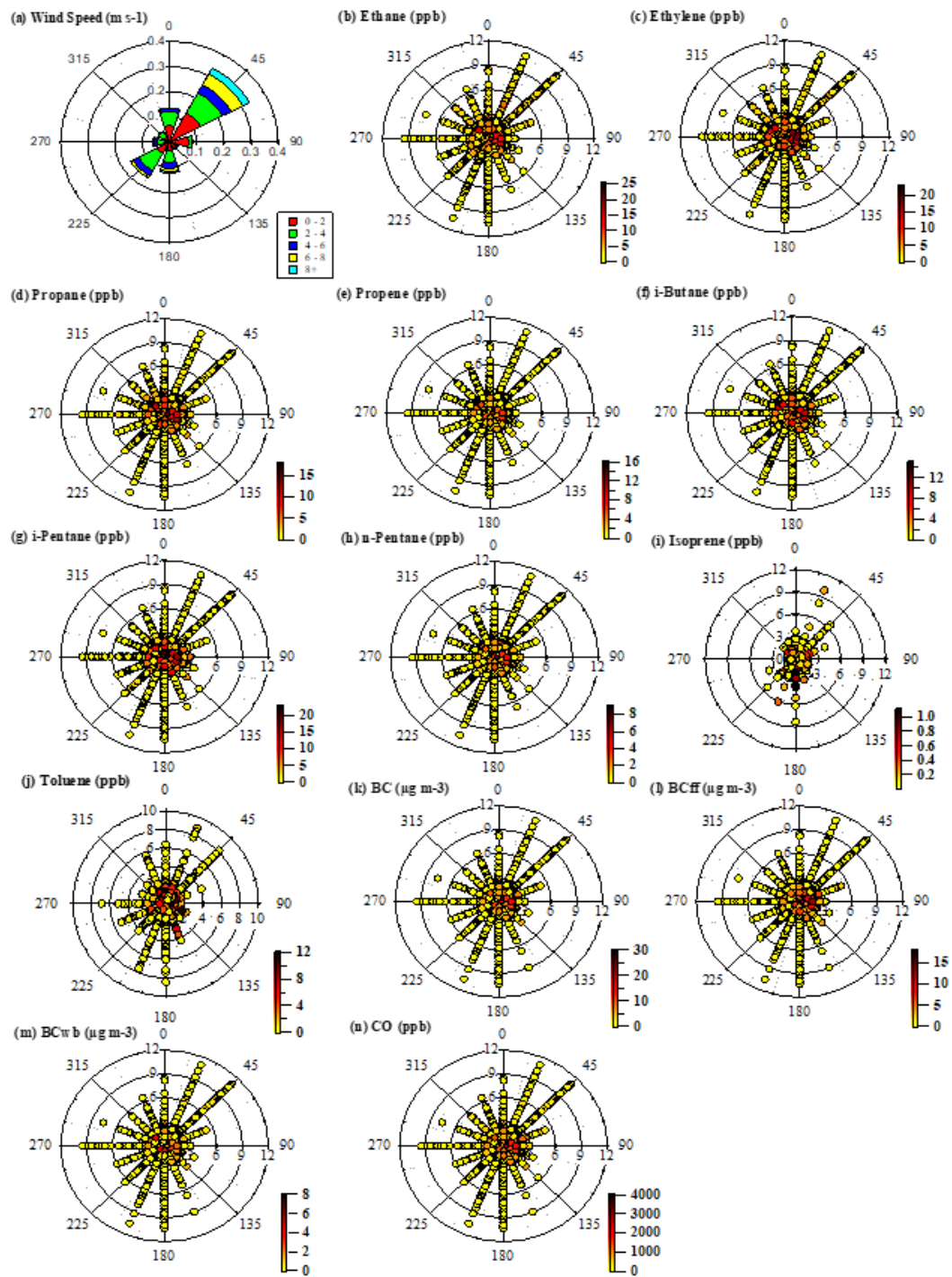
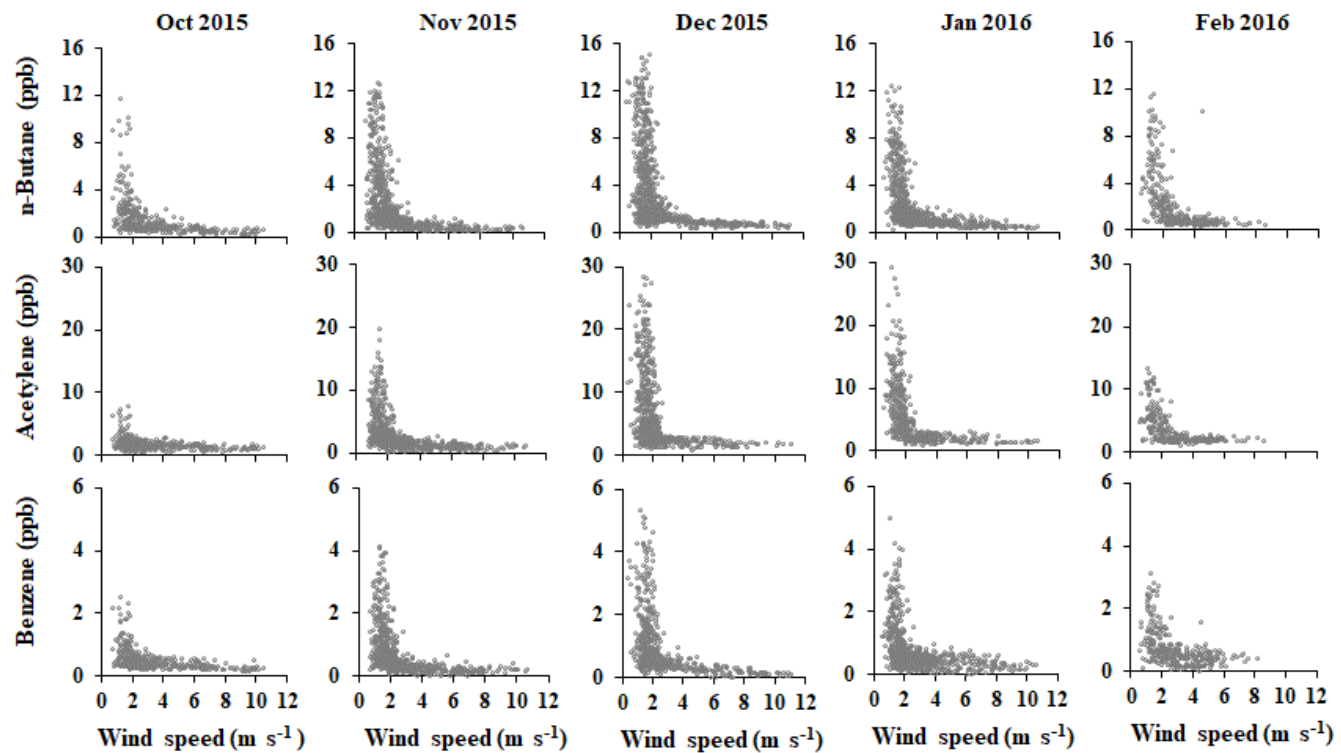


Figure S5. Monthly variability of n-butane, acetylene and benzene relatively to wind speed.

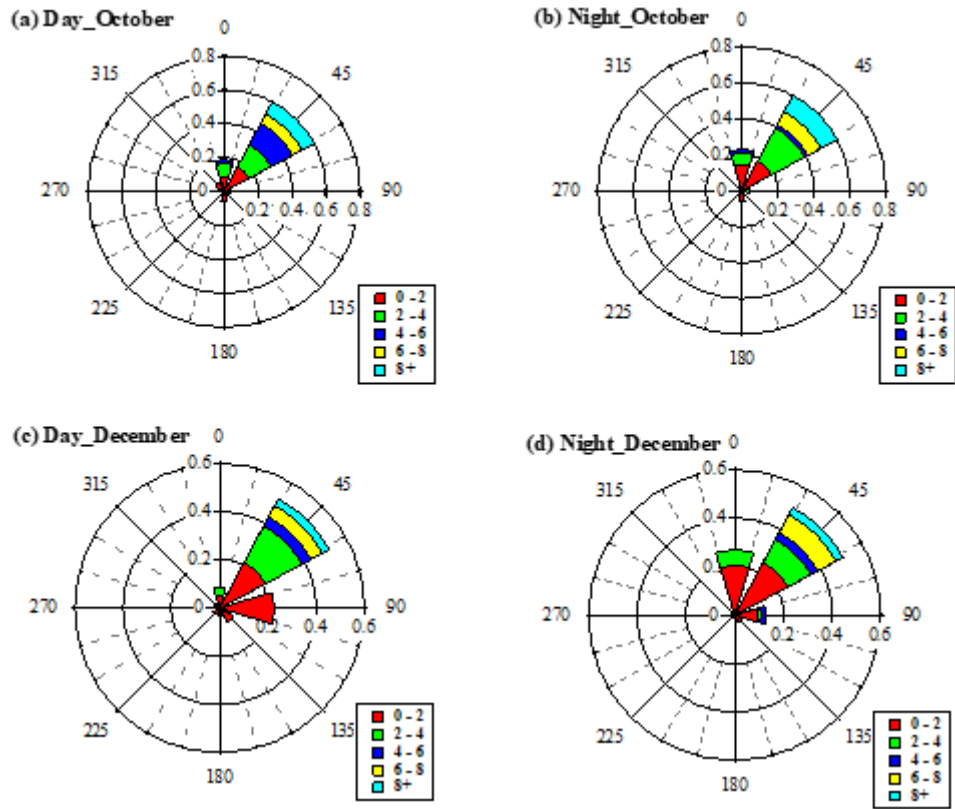


5

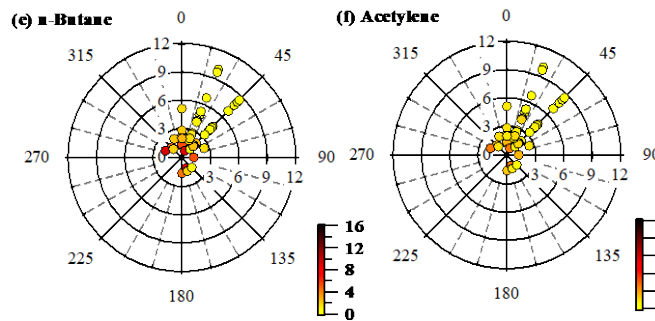
10

15

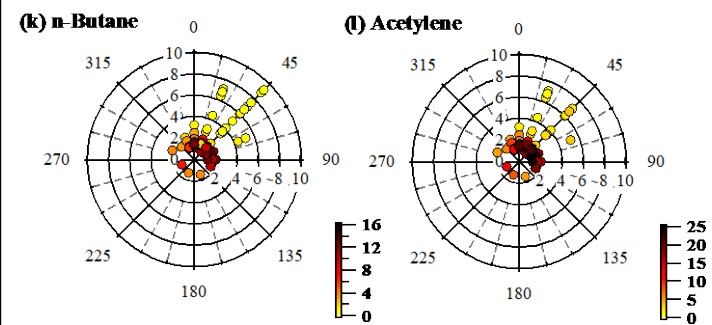
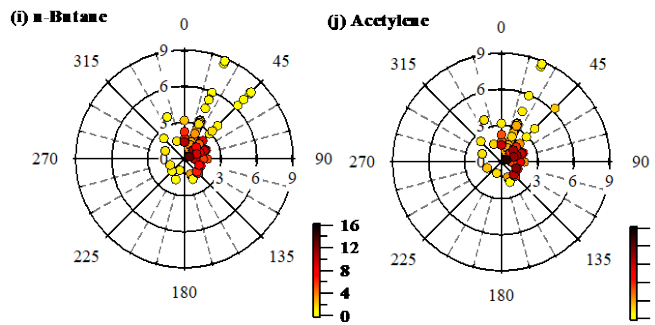
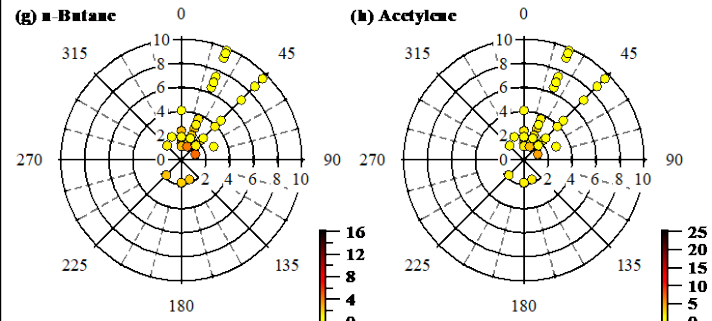
Figure S6. Wind roses for Thissio station for the morning hours (07:00 – 09:00) and night hours (21:00 – 23:00) of October (a-b) and December (c-d); concentration roses of n-butane and acetylene for October morning (07:00 – 09:00) (e-f), October night (21:00 – 23:00) (i-j), December morning (07:00 – 09:00) (g-h) and December night (21:00 – 23:00) (k-l) respectively.



October - DAY



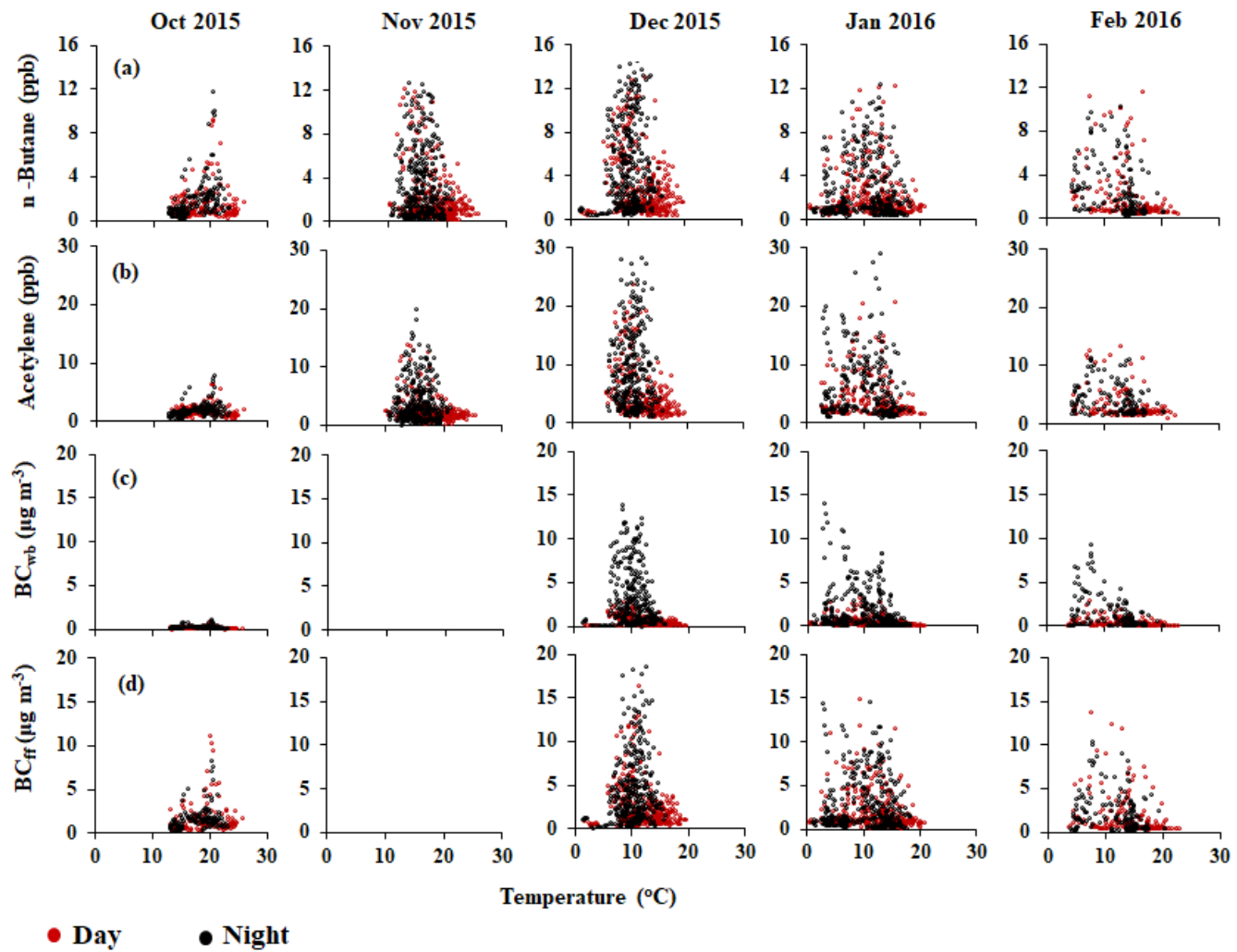
October - NIGHT



December- DAY

December- NIGHT

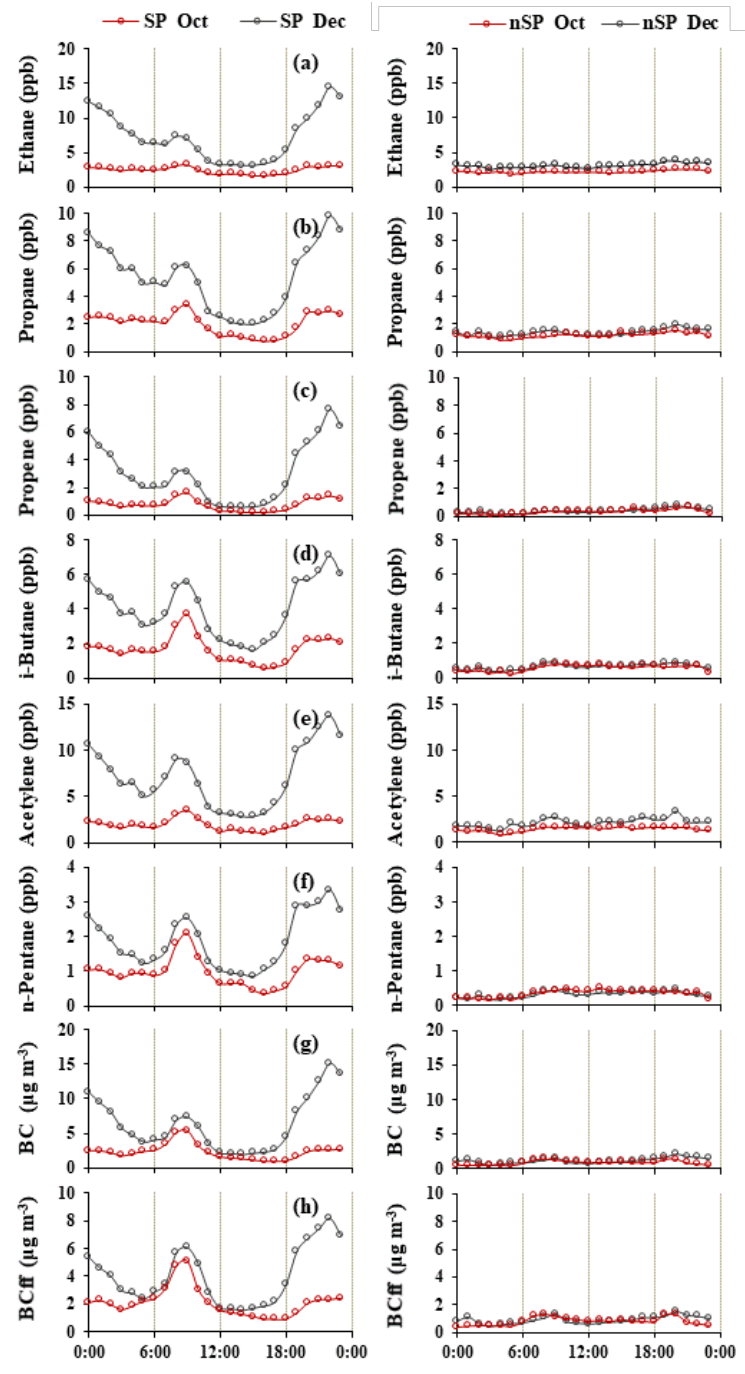
Figure S7. Monthly variability of (a) n-butane, (b) acetylene, (c) BC_{wb} and (d) BC_{ff} against temperature for the period 16 October 2015 - 15 February 2016 at Thissio urban background site.



5

10

Figure S8. Diurnal patterns of (a) ethane, (b) propane, (c) propene, (d) i-butane, (e) acetylene, (f) n-pentane, (g) BC and (h) BC_{ff} during the SP (left column) and the nSP (right column) periods identified during October 2015 (red) and December 2015 (black) respectively. Note: SP periods are defined by wind-speed lower than 3 ms^{-1} and absence of rainfall, while nSP periods are defined by winds-speeds higher than 3 m s^{-1} .



Section S.2.% Mass contribution of the measured NMHCs in the morning peak (Sect. 3.4.3, Fig. 9).

The morning profile of NMHCs at Thissio station was obtained from the measurements of specific SP days of January and February 2016, due to TEX availability. **The first step of the procedure is the conversion of the NMHC concentrations from ppb to $\mu\text{g m}^{-3}$, based on Eq. (S1):**

$$5 \quad C_i(\mu\text{g m}^{-3}) = C_i(\text{ppb}) \times \frac{M_i}{24} \quad (\text{S1})$$

where $C_i(\mu\text{g m}^{-3})$ is the calculated concentration of the compound i in $\mu\text{g m}^{-3}$, $C_i(\text{ppb})$ is the concentration of the compound i in ppb, M_i is the molar mass of the compound in g mol^{-1} and the number 24 is the molecular volume of the ideal gas in 1atm and ambient temperature 25°C.

The next step is the calculation of the baseline level that will be subtracted by the morning maximum value in order to minimize the contribution of other sources besides traffic. This is important because the shape of the morning peak is not very clear, as it is depicted in Fig. S9 for i-pentane (motor vehicle exhaust marker, Baudic et al., 2016) for a representative day from the studied period.

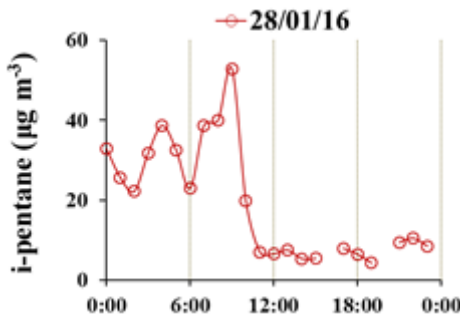


Figure S9. Daily variability of i-pentane for the 28/01/2016.

15

As a result, the baseline level is given from Eq. (S2), as the average of the measured concentrations at the beginning and the end of the morning peak:

$$C_{baseline,i} = \frac{C_{6,i} + C_{11,i}}{2}, \quad (\text{S2})$$

where $C_{baseline,i}$ is the calculated baseline level for the compound i in $\mu\text{g m}^{-3}$, $C_{6,i}$ is the concentration of the compound i at 06:00LT and $C_{11,i}$ is the concentration of the compound i at 11:00LT.

Subsequently, the mass contribution of each NMHC for the morning peak is calculated from Eq. (S3):

$$MassContribution_i = \frac{C_{morning,i} - C_{baseline,i}}{\sum_{i=1}^n C_i^*}, \quad (S3)$$

where $MassContribution_i$ is the calculated contribution of the compound i to the total mass of compounds, $C_{morning,i}$ is the maximum morning concentration of the compound i between 07:00 - 10:00LT, $C_{baseline,i}$ is the baseline level of the compound i calculated by the Eq. (S2) and C_i^* is the result of the subtraction of the $C_{baseline,i}$ from the $C_{morning,i}$ for a compound i .

For the morning profile of NMHCs at Patission station the same approach was adapted for the subtraction of the baseline, however, due to the small number of samples, the concentrations of the 06:55 sample were taken as the baseline level. Consequently, the mass contribution of each NMHC for the morning peak of Patission is calculated from Eq. (S4):

$$10 \quad MassContribution_i = \frac{C_{morning,i} - C_{baseline,i}}{\sum_{i=1}^n C_i^*}, \quad (S4)$$

where $MassContribution_i$ is the calculated contribution of the compound i to the total mass of compounds, $C_{morning,i}$ is the maximum morning concentration of the compound i (in $\mu\text{g m}^{-3}$) between 08:00 - 10:00LT, $C_{baseline,i}$ is concentration of the compound i of the 06:55 sample (in $\mu\text{g m}^{-3}$) and C_i^* is the result of the subtraction of the $C_{baseline,i}$ from the $C_{morning,i}$ for a compound i .

15

Section S.2a. Tunnel measurements (Sect. 3.4.3, Fig. 9).

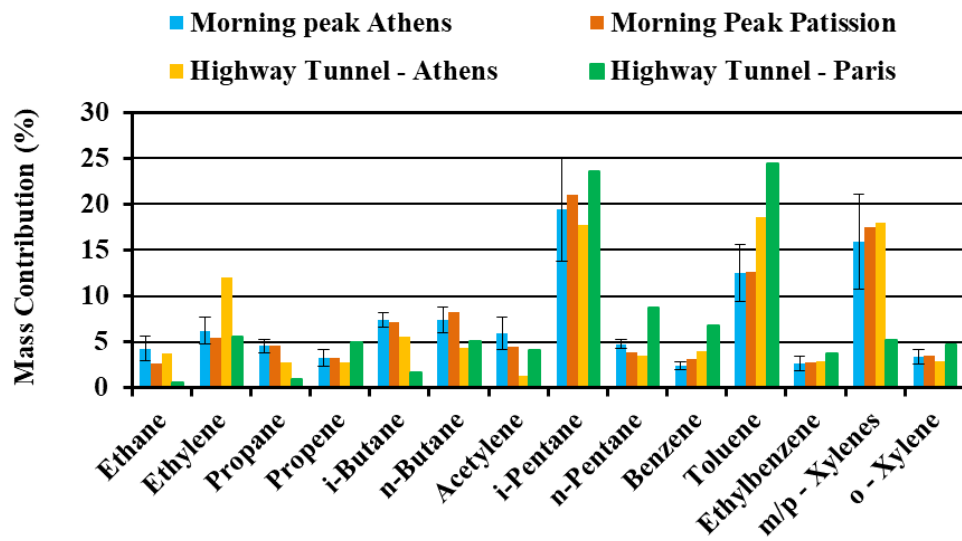
Apart from the street canyon measurements described in Sect. 2.4 and Sect. 3.4.3, NMHCs measurements were also conducted in a tunnel at the peripheral highway of Athens, (Attiki Odos), on 12 May 2016 from 12:00 LT to 12:45 LT (LT = UTC+2), to identify the NMHCs fingerprint of traffic emissions. The tunnel's length is 200 m with 3 lanes at each direction and no specific restrictions for heavy duty vehicles. Each driving direction consists of a separated compartment and a ventilation system was installed but not operated. The measurements are performed at the middle of the tunnel length to avoid as much as possible the influence of ambient air from outside. For the sampling 6L stainless steel – silonite canisters were used and the sampling time ranged between 2 and 10 minutes. The sampling method for ambient air is described in details elsewhere (Sauvage et al., 2009). Before the analysis, the cylinders were pressurized by adding a known amount of zero-air resulting in a sample dilution by a factor of two. Afterwards each canister was connected to the GC-FID system using a Teflon (PTFE) sampling line and analyzed by the method described in Sect. 2.2. Before sampling, the canisters were cleaned by filling them up with zero air and re-evacuated, at least three times. The content of the cylinders was then analyzed by the GC-FID system to verify the efficiency of the cleaning procedure. The canisters were evacuated a few days prior to the use and they were analyzed maximum 1 day after the sampling.

To complement the analysis and explanation of the morning peak observed in Thissio and Patission measurements, in Sect. 3.4.3 we compare the mass contribution (%) of NMHCs in the mentioned morning profiles (Sect. 3.4.3, Fig. 9), with the profile derived from the tunnel measurements in Athens (Highway Tunnel - Athens), as well as the profile derived from tunnel measurements conducted 20 Km southern of the center of Paris (France) in autumn 2012 (Highway Tunnel – Paris) 5 (Fig. S10).

The profile of the tunnel measurements of Athens derives as follows: First of all, the NMHC concentrations are converted from ppb to $\mu\text{g m}^{-3}$, based on Eq. (S1). Secondly, the mass contribution of each NMHC for the Athens Tunnel Profile of is calculated from Eq. (S5):

$$\text{Mass Contribution}_i = \frac{C_i}{\sum_{i=1}^n C_i}, \quad (\text{S5})$$

10 where $\text{Mass Contribution}_i$ is the calculated contribution of the compound i to the total mass of compounds, and C_i is the mean concentration of the compound i (in $\mu\text{g m}^{-3}$) in the samples of 12:05 & 12:40 LT. Due to the small number of samples a baseline subtraction from the tunnel data was not possible.



15 **Figure S10. % Mass contribution of the measured NMHCs during the morning peak (07:00 – 10:00 LT), median values in Thissio, mean values in Patission Monitoring Station, in a highway tunnel in GAA and a highway tunnel close to Paris.**

The tunnel profiles present a lot of common features as well as a few large discrepancies ($R^2 = 0.53$), despite the different 20 conditions associated with their profiles (Paris versus Athens, tunnel length, season etc). Again i-pentane and toluene are the two main compounds of the profiles at least in Athens accounting for about 54% of the total measured NMHCs, followed by

n -butane, ethylene and benzene accounting for almost 20% at both sites. The most striking difference between the two tunnels concerns ethylene (factor of 2 higher in Athens compared to Paris), acetylene (factor of 3 lower in Athens compared to Paris), i-butane (factor of 3 lower in Paris than Athens), n-pentane (almost a factor of two higher in Paris compared to Athens) and m-/p- xylenes (almost a factor of 3 lower in Paris compared to Athens). The biggest difference between the two 5 Athens morning peaks and Athens tunnels concerns acetylene and toluene (factor of 4 and 1.5 respectively). The above similarities and differences can be attributed to the car-fleet and the type of fuel used, as it is described in Sect. 3.4.3 of the manuscript.

Section S.3. Investigation of the evaporation losses (Sect. 3.4.3, Fig. 9).

10 In Sect. 3.4.3, the increased mass contribution of butanes and propane to the morning profiles of Thissio and Patission was attributed to LPG fuels, thus to fuel evaporation. To better investigate this possibility, we followed a similar approach as Na and Kim (2001) for Seoul (South Korea), in order to examine the relationship of the ratio Butanes-to-(C2 – C5)Alkanes (%) and temperature for every month (Fig. S11). More specifically, the ratio of the sum of i-butane and n-butane versus the sum 15 of ethane, propane, i-butane, n-butane, i-pentane and n-pentane for every sample was calculated. Ethylene, propene and acetylene are excluded from this ratio due to their reactivity. The mean and standard deviation values of the ratio were derived for the temperatures between 1°C to 25°C (minimum and maximum of the period respectively). These values were plotted against the temperature for each month. The highest values of the ratio are observed for high temperatures and the lowest for low ambient temperature, although the standard deviation is considerable. It is interesting to note that the same pattern occurs when the ratio Pentanes-to-(C2 – C5)Alkanes (%) versus the temperature is examined (Fig. S12). Taking into 20 account the positive dependence of the two ratios to temperature, we can assume that fuel evaporation losses are also an important source of NMHCs. In addition, the above results could indicate why the Athens tunnel results performed in May differ from Patission and Thissio winter morning profiles.

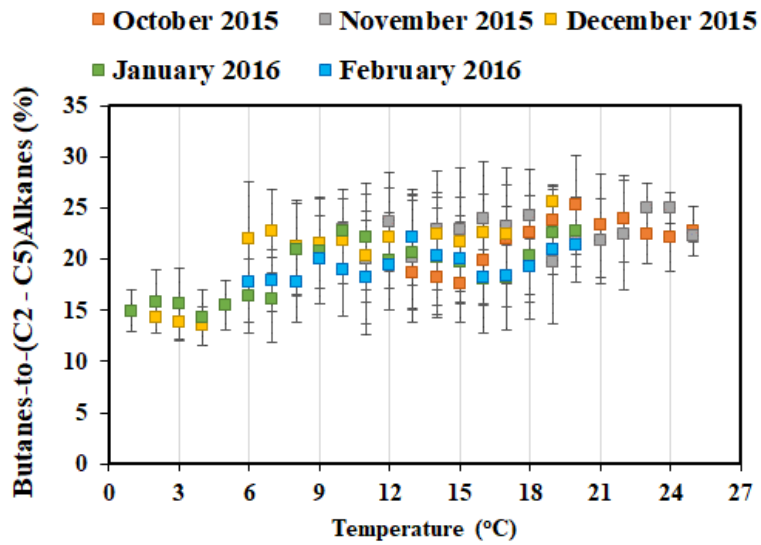


Figure S11. Scatter plots of the ratio Butanes-to-(C2 – C5)Alkanes (%) to temperature for October 2015, November 2015, December 2015, January 2016 and February 2016.

5

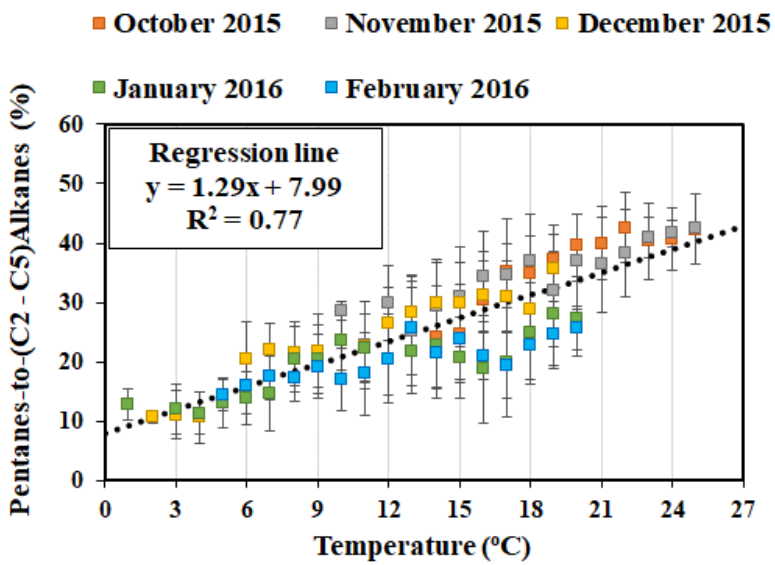
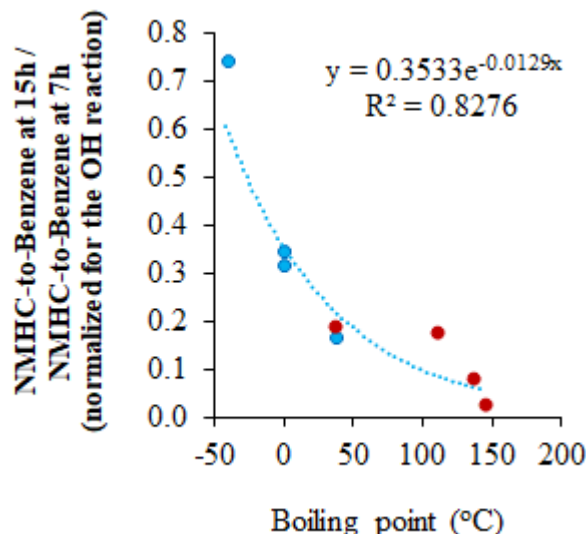


Figure S12. Scatter plots of the ratio Pentanes-to-(C2 – C5)Alkanes (%) to temperature for October 2015, November 2015, December 2015, January 2016 and February 2016.

10

Furthermore, it is important to mention that Kourtidis et al., (1999) also performed an investigation of the evaporative emissions for Athens with data obtained at a street canyon location (Patission station) in September 1994. To compare our observations from Thissio station with those reported by Kourtidis et al., (1999), the ratio of NMHC/benzene at 15:00 and 07:00 (normalized to the OH reactions) versus the boiling point of selected NMHC was examined, using our data from 5 Thissio station (Fig. S.13). To include more common NMHC with Kourtidis et al., (1999), we used data from 21 January to 15 February 2016, when toluene, ethylbenzene and o-xylene are additionally available. The selected data had wind speed less than 2.8 m s^{-1} to maximize impact from local sources, while at 07:00 and 15:00 LT the mean temperature was approximately 8°C and 12.5°C respectively. Although the examined periods have discrepancies in ambient temperature (winter is colder than autumn), the exponential curve fitting of our data ($y = 0.3533e^{-0.0129x}$, where x is the boiling point in 10 $^\circ\text{C}$) is very close to the one reported in Kourtidis et al., (1999) ($y = 0.44e^{-0.0118212T}$, where T is the boiling point in $^\circ\text{C}$).



15 **Figure S13. Ratios of the NMHC/benzene ratio for 15:00 and 07:00 to the boiling points of the selected NMHC, divided by the reaction rate constant of each species with OH. The plotted NMHC are propane, i-/n- butane, i-/n- pentane, toluene, ethylbenzene and o-xylene. The red cycles indicate compounds (not values) in common with the work of Kourtidis et al., (1999).**

Finally, we examine the monthly variation of i-butane relatively to n-butane (Fig. S14). The two compounds have linear relationship with no significant temporal differences on the slopes (only October and December equations are presented). In 20 addition, the regression is similar to the one derived from the Patission measurements (depicted on Fig. S14), thus supporting our assumption that the observations are traffic related.

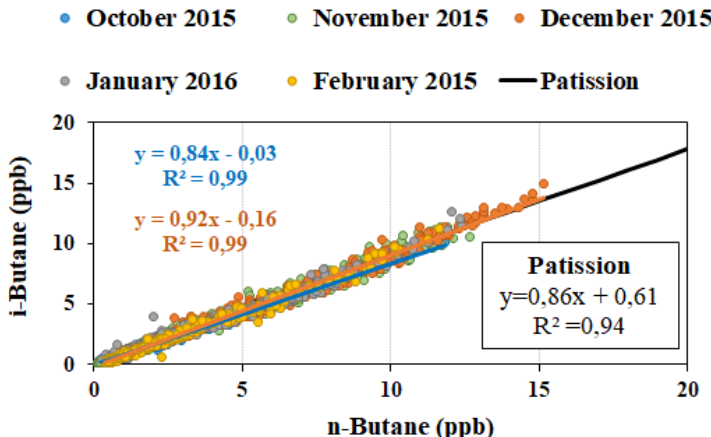


Figure S14. Scatter plots between i-butane relatively to n-butane for October 2015, November 2015, December 2015, January 2016 and February 2016 for the Thissio site. The black line corresponds to the Patission data regression.

5 Section S.4. %Mass contribution of the measured NMHCs in the night-time enhancement period (Sect. 3.4.3, Fig. 11).

The night profile of NMHCs at Thissio station was obtained from the measurements of specific SP nights of October and December 2015, due to their different temperature condition (October is warmer than December) that influence the need for residential heating. **The first step of the procedure is the conversion of the NMHC concentrations from ppb to $\mu\text{g m}^{-3}$, based on Eq. (S1).**

10 The next step is the determination of the baseline level that will be subtracted by the night maximum value (between 22:00 and 23:00 LT) as it is also seen in Fig. 4 and Fig. 8. For that purpose, the minimum concentration of each compound between 12:00 LT – 17:00 LT is used.

Subsequently, the mass contribution of each NMHC for the night peak is calculated from Eq. (S6):

$$MassContribution_i = \frac{C_{night,i} - C_{baseline,i}}{\sum_{i=1}^n C_i^*}, \quad (S6)$$

15 where $MassContribution_i$ is the calculated contribution of the compound i to the total mass of compounds, $C_{night,i}$ is the maximum night concentration of the compound i (in $\mu\text{g m}^{-3}$) between 22:00 - 23:00 LT, $C_{baseline,i}$ is the minimum concentration of the compound i (in $\mu\text{g m}^{-3}$) for the same date between 12:00 – 17:00 LT and C_i^* is the result of the subtraction of the $C_{baseline,i}$ from the $C_{night,i}$ for a compound i .

References

Baudic, A., Gros, V., Sauvage, S., Locoge, N., Sanchez, O., Sarda-Estève, R., Kalogridis, C., Petit, J.-E., Bonnaire, N., Baisnée, D., Favez, O., Albinet, A., Sciare, J. and Bonsang, B.: Seasonal variability and source apportionment of volatile organic compounds (VOCs) in the Paris megacity (France), *AtmosChem Phys*, 16(18), 11961–11989, doi:10.5194/acp-16-11961-2016, 2016.

Kourtidis, K. A., Ziomas, I. C., Rappenglueck, B., Proyou, A. and Balis, D.: Evaporative traffic hydrocarbon emissions, traffic CO and speciated HC traffic emissions from the city of Athens, *Atmos. Environ.*, 33(23), 3831–3842, doi:10.1016/S1352-2310(98)00395-1, 1999.

10 Na, K. and Kim, Y. P.: Seasonal characteristics of ambient volatile organic compounds in Seoul, Korea, *Atmos. Environ.*, 35(15), 2603–2614, 2001.